


# Feeding state regulates pheromone-mediated avoidance behavior via the insulin signaling pathway in *Caenorhabditis elegans*

Leesun Ryu<sup>1</sup>, Yongjin Cheon<sup>1</sup>, Yang Hoon Huh<sup>2</sup>, Seondong Pyo<sup>1</sup>, Satya Chinta<sup>3</sup>, Hongsoo Choi<sup>4</sup>,  
Rebecca A Butcher<sup>3</sup> & Kyuhyung Kim<sup>1,\*</sup> 

## Abstract

Animals change sensory responses and their eventual behaviors, depending on their internal metabolic status and external food availability. However, the mechanisms underlying feeding state-dependent behavioral changes remain undefined. Previous studies have shown that *Caenorhabditis elegans* hermaphrodite exhibits avoidance behaviors to acute exposure of a pheromone, *ascr#3* (*asc-ΔC9*, C9). Here, we show that the *ascr#3* avoidance behavior is modulated by feeding state via the insulin signaling pathway. Starvation increases *ascr#3* avoidance behavior, and loss-of-function mutations in *daf-2* insulin-like receptor gene dampen this starvation-induced *ascr#3* avoidance behavior. DAF-2 and its downstream signaling molecules, including the DAF-16 FOXO transcription factor, act in the *ascr#3*-sensing ADL neurons to regulate synaptic transmission to downstream target neurons, including the AVA command interneurons. Moreover, we found that starvation decreases the secretion of INS-18 insulin-like peptides from the intestine, which antagonizes DAF-2 function in the ADL neurons. Altogether, this study provides insights about the molecular communication between intestine and sensory neurons delivering hunger message to sensory neurons, which regulates avoidance behavior from pheromones to facilitate survival chance.

**Keywords** avoidance behavior; DAF-2 insulin receptor; feeding state; pheromone; synaptic transmission

**Subject Categories** Cancer; Signal Transduction; Transcription

DOI 10.15252/emboj.201798402 | Received 11 October 2017 | Revised 10 May 2018 | Accepted 15 May 2018 | Published online 19 June 2018

The EMBO Journal (2018) 37: e98402

## Introduction

Acute and chronic adaptations to the ever-changing external and internal environments are crucial for animal survival. Internal

metabolic status induced by satiety and hunger has been shown to modulate animal physiology and behavior (see review Mayer, 2011). Particularly, depending on feeding status, animals change sensory responses, leading to altered behavioral outcomes (Magni *et al*, 2009; Nassel & Winther, 2010; Palouzier-Paulignan *et al*, 2012). These effects of feeding state on the sensory system have been widely reported in invertebrate and vertebrate systems. For example, increased food intake reduces monkey visual responses, causing decreased behavioral response to food sources (Critchley & Rolls, 1996). In another example, starvation promotes food-seeking behavior via direct modulation of *Drosophila* olfactory neurons (Root *et al*, 2011). However, molecular or circuit mechanisms underlying feeding state-regulated sensory responses still remain largely uncharacterized.

The nematode *Caenorhabditis elegans* has a well-defined nervous system with only 302 neurons that mediate a broad spectrum of sensory behaviors, such as chemosensation, nociception, thermosensation, foraging, and feeding. These behaviors are plastic and can be modulated by the animal's feeding state (see review Sengupta, 2013). For example, acute starvation alters patterns of locomotion and decreases the rates of pharyngeal pumping and egg laying (Trent *et al*, 1983; Avery & Thomas, 1997; Sawin *et al*, 2000; Hills *et al*, 2004). In addition, the presence or absence of food acutely affects chemosensory behaviors; presence of food enhances avoidance behavior to repulsive chemicals (Ezcurra *et al*, 2011), whereas absence of food increases adaptation to repeated exposure of attractive odorants and noxious soluble chemicals, including copper and glycerol (Colbert & Bargmann, 1997; Ezcurra *et al*, 2016). Chronic starvation has shown to also affect chemosensory behaviors and gene expression of chemosensory signaling genes (Saeki *et al*, 2001; Gruner *et al*, 2014, 2016). However, little is known about the mechanisms underlying starvation-mediated changes of chemosensory behaviors.

Insulin level reflects feeding state of an animal and directly regulates sensory responses (Fadool *et al*, 2000; Lacroix *et al*, 2008). In *Drosophila*, starvation increases attractive behaviors to favorable

1 Department of Brain and Cognitive Sciences, DGIST, Daegu, Korea

2 Electron Microscopy Research Center, Korea Basic Science Institute, Cheongju-si, Chungcheongbuk-do, Korea

3 Department of Chemistry, University of Florida, Gainesville, FL, USA

4 Robotics Engineering Department, DGIST, Daegu, Korea

\*Corresponding author. Tel: +82 53 785 6124; E-mail: khkim@dgist.ac.kr

odors and decreases avoidance behaviors to unfavorable odors via the change of neuronal activities in the olfactory neurons by regulating insulin signaling (Root *et al*, 2011; Ko *et al*, 2015). In *C. elegans*, INS-1, an insulin-like peptide, regulates olfactory response to odors and thus affects their olfactory behavior (Chalasan *et al*, 2010). However, a systemic analysis to investigate how insulin signaling regulates the sensory behavior by food availability in the whole organism context has not been performed yet.

*Caenorhabditis elegans* produces a complex pheromone mixture composed of small chemicals called ascarosides. Subsets of ascarosides have been shown to regulate many aspects of nematode development and behavior including dauer formation and sensory perception (Jeong *et al*, 2005; Butcher *et al*, 2007; Edison, 2009; Macosko *et al*, 2009). Previously, we showed that adult hermaphrodites exhibit acute avoidance to the ascaroside *ascr#3*, which is mediated by the nociceptive ADL neurons (Jang *et al*, 2012). Moreover, early experience of *ascr#3* modulates *ascr#3* avoidance as adults, indicating that *ascr#3* avoidance behaviors are plastic (Hong *et al*, 2017).

Here, we show that *ascr#3* avoidance is further modulated by feeding state. We found that prolonged starvation enhances *ascr#3* avoidance behaviors of adult hermaphrodites. DAF-2 insulin-like signaling acts in the ADL *ascr#3*-sensing neurons to mediate starvation-induced *ascr#3* avoidance by upregulation of the expression level of synaptic molecules via DAF-16 FOXO. Moreover, we also found that prolonged starvation inhibits secretion of an insulin-like peptide INS-18 from the intestine, which antagonizes the function of DAF-2 in ADL. Taken together, these results indicate that prolonged starvation affects the secretion of intestinal insulin-like peptides, which may function via a DAF-2 receptor to regulate the synaptic output of pheromone-sensing neurons and thus the pheromone avoidance behavior.

## Results

### Starvation alters avoidance behaviors to *ascr#3* via the DAF-2 insulin-like receptor

To investigate whether *ascr#3* avoidance behaviors are affected by feeding state, we fed or starved young adult animals for 3, 6, or 24 h and examined acute avoidance to 100 nM *ascr#3* (Fig 1A). We found that animals starved for longer than 6 h showed

increased *ascr#3* avoidance, compared to animals well-fed and animals starved for only 3 h (Fig 1B). Increased *ascr#3* avoidance appeared to be mediated by increased long reversals but not short reversals or omega turns in starved animals (Fig EV1A; Hong *et al*, 2017). The increased *ascr#3* avoidance in the animals starved for 6 h was reversed to normal level, after 24 h of re-feeding (Fig 1C). To further examine the effects of starvation on *ascr#3* avoidance, we tested *eat-2* loss-of-function mutant animals. *eat-2* encodes nicotinic acetylcholine receptor subunit of which mutations cause decreased pharyngeal pumping, resulting in a dietary restriction state (Lakowski & Hekimi, 1998; Lopez *et al*, 2013). We found that *ascr#3* avoidance was increased in *eat-2* mutants, similar to that of wild-type animals starved for 6 h (Fig EV1B). These results indicate that feeding state influences avoidance behavior to *ascr#3*.

Since DAF-2/insulin-like signaling has been reported to modify effects of dietary restriction (Lemieux & Ashrafi, 2015), we investigated whether DAF-2 regulates starvation-mediated increase in *ascr#3* avoidance. We tested *ascr#3* avoidance of *daf-2(e1370)* reduction-of-function mutants under well-fed and starved conditions (Kimura *et al*, 1997) and found that this mutation not only suppressed increased *ascr#3* avoidance in animals starved for 6 h or 24 h, but also decreased *ascr#3* avoidance in well-fed animals (Fig 1D and E). *ascr#3* avoidance was also decreased in well-fed *daf-2(e1368)* mutant animals carrying another reduction-of-function allele (Fig EV1C). In addition, *daf-2* mutation suppressed the enhancement of *ascr#3* avoidance in *eat-2* mutants (Fig EV1B). Furthermore, increased *ascr#3* avoidance in the presence of food was also abolished in *daf-2* mutants (Fig EV1D; Jang *et al*, 2012). These results suggest that DAF-2/insulin-like signaling modulates feeding state-dependent alteration of *ascr#3* avoidance.

We next examined where DAF-2 acts to control *ascr#3* avoidance. We expressed *daf-2* cDNA under the control of upstream regulatory sequences of *unc-14* (pan-neuronal; Ogura *et al*, 1997) or *sre-1* (ADL marker) gene (Fig EV1E; Jang *et al*, 2012; Gruner *et al*, 2014; Hong *et al*, 2017). Pan-neuronal expression or ADL-specific expression of *daf-2* cDNA fully rescued the defects of *ascr#3* avoidance in *daf-2* mutants (Fig 1F). Moreover, the expression of *daf-2* cDNA in ADL also restored increased avoidance behaviors to *ascr#3* in animals starved for 6 h or 24 h (Fig 1G). Taken together, these observations indicate that DAF-2/insulin-like signaling acts in the *ascr#3*-sensing ADL neurons to regulate *ascr#3* avoidance behaviors in a feeding state-dependent manner.

#### Figure 1. An insulin/IGF-1-like receptor, *daf-2*, is required for increase in *ascr#3* avoidance under starvation conditions.

- A Experimental scheme of *ascr#3* avoidance assay depending upon starvation. 50–100 young adult animals are washed and placed on seeded (fed: colored in black) or non-seeded (starved: colored in gray) plates for each duration: 3, 6, and 24 h; then, various concentrations of *ascr#3* are delivered to the front of a freely moving forward animal to measure avoidance frequencies responding to *ascr#3*.
- B Fraction reversing of fed and starved animals in response to *ascr#3* exposure.  $n = 50\text{--}70$ .  $***P < 0.001$  and  $****P < 0.0001$  (one-way ANOVA Bonferroni's test).
- C Fraction reversing of re-fed animals from 6-h starvation in response to *ascr#3* exposure. A 24-h re-feeding period reverses *ascr#3* avoidances to well-fed status.  $n = 40\text{--}80$ .  $*P < 0.05$  (one-way ANOVA Dunnett's Test).
- D Fraction reversing of *daf-2* mutant animals in fed and starved status in response to *ascr#3* exposure.  $n = 40\text{--}60$ .
- E Fraction reversing of well-fed wild-type animals and *daf-2* mutants in response to 100, 200, and 400 nM *ascr#3*.  $n = 60$ .  $***P < 0.001$  (Bonferroni's test).
- F Fraction reversing of wild-type animals, *daf-2* mutants, and *daf-2* mutants expressing *unc-14p::daf-2* cDNA (neurons) or *sre-1p::daf-2* cDNA (ADL) in response to 500 nM *ascr#3*. *daf-2* cDNA expression in neuron and ADL restores the defect of *ascr#3* avoidance in *daf-2* mutants.  $n = 60$ .  $*P < 0.05$  (Dunnett's test).
- G Fraction reversing of wild-type animals, *daf-2* mutants, and *daf-2* mutants expressing *sre-1p::daf-2* cDNA (ADL) in fed and starved conditions in response to *ascr#3*.  $n = 40\text{--}70$ .  $**P < 0.01$  and  $****P < 0.0001$  (Bonferroni's test).

Data information: All error bars represent  $\pm$  SEM.

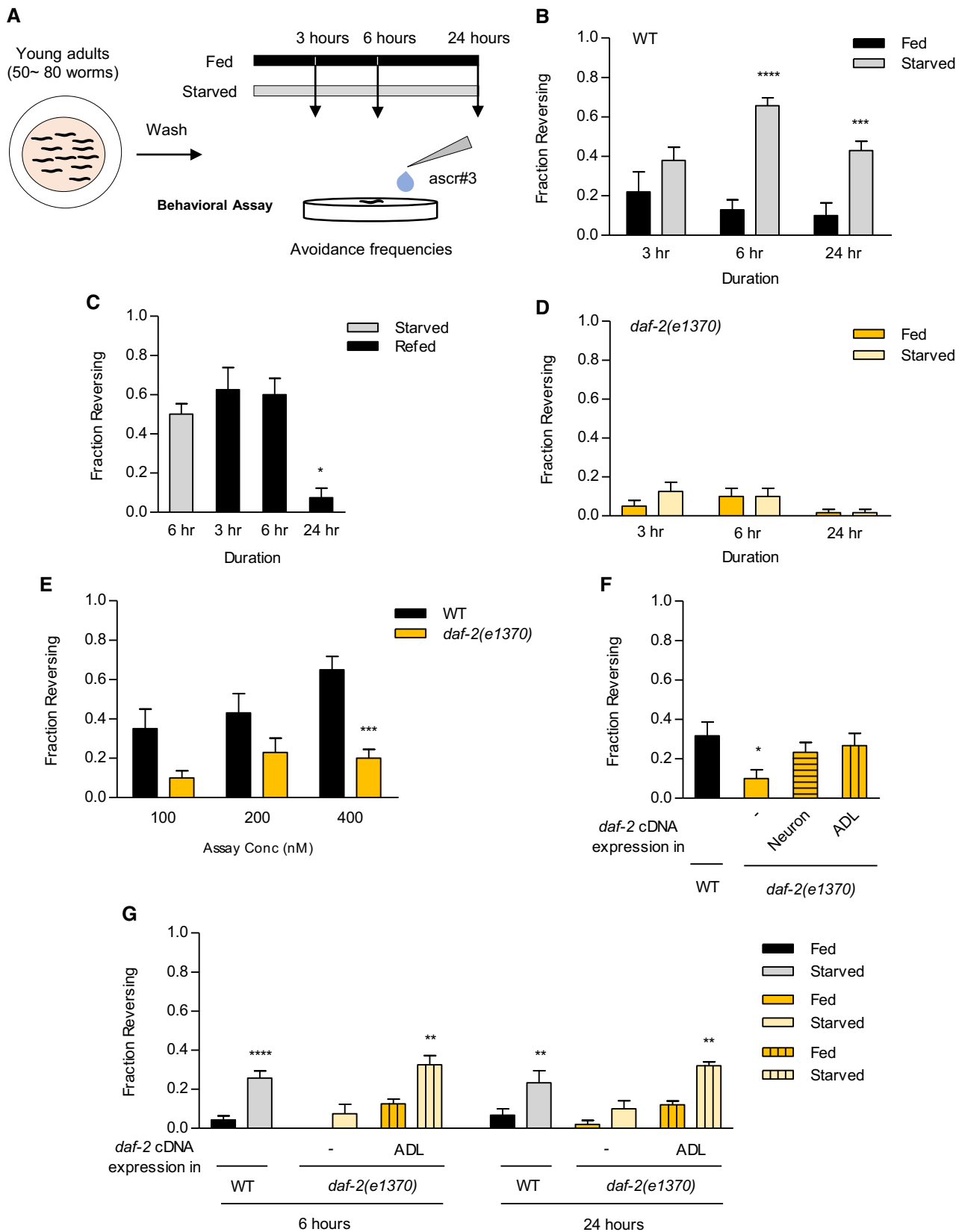


Figure 1.

### DAF-2 signaling mediates Ca<sup>2+</sup> responses, not in the ADL sensory neurons, but in the AVA interneurons upon *ascr#3* exposure

Previously, works showed that ADL neurons exhibit transient Ca<sup>2+</sup> responses to acute *ascr#3* exposure in a dose-dependent manner (Jang *et al.*, 2012). Therefore, altered *ascr#3* avoidance in *daf-2* mutants may be due to decreased ADL Ca<sup>2+</sup> responses to *ascr#3* exposure. In order to test the hypothesis, we measured the intracellular Ca<sup>2+</sup> dynamics of ADL upon *ascr#3* exposure using the genetically encoded calcium sensor GCaMP3 (Chronis *et al.*, 2007; Jang *et al.*, 2012). We found that the Ca<sup>2+</sup> activities of ADL were unaltered in *daf-2* mutants, compared to wild-type animals, when animals were exposed to either 100 nM or 500 nM *ascr#3* (Fig 2A). Previously, it was shown that Ca<sup>2+</sup> transients of ADL upon *ascr#3* exposure were not affected by starvation for 6 h (Gruner *et al.*, 2014). These results indicate that the loss of DAF-2 and starvation for 6 h do not affect sensory response of ADL to *ascr#3*.

The ADL sensory neurons form chemical synapses onto the AVA, AVD, and AIB interneurons, which trigger backward movements by activating DA or VA motor neurons (Chalfie *et al.*, 1985; White *et al.*, 1986). The signals from ADL neurons mainly transit to AVA but not AVD and AIB upon *ascr#3* exposure (Hong *et al.*, 2017). Thus, we next monitored Ca<sup>2+</sup> transients of AVA in *daf-2* mutants and found that the Ca<sup>2+</sup> transients of AVA upon *ascr#3* exposure were abolished in *daf-2* mutants. Similar to the *ascr#3* avoidance defects, *ascr#3* Ca<sup>2+</sup> transient defects in *daf-2* mutants were fully rescued by *daf-2* cDNA expression in ADL (Fig 2B and C), indicating that DAF-2 acts in ADL to regulate *ascr#3* responses of the ADL downstream target neurons.

### DAF-2 signaling regulates chemical synaptic transmission from ADL

The finding that loss of DAF-2 function decreases *ascr#3* responses in ADL downstream neurons prompted us to examine the effects of DAF-2 signaling on chemical synaptic transmission from ADL. We first examined synaptic densities in the ADL neurons by expressing functional YFP-tagged SNB-1/synaptobrevin, which is a component of SNARE (soluble NSF attachment protein receptor) proteins and has been used as a pre-synaptic marker in *C. elegans* (Nonet *et al.*, 1998; Shen & Bargmann, 2003; Sieburth *et al.*, 2005; Noma & Jin, 2015). We measured fluorescence intensity of SNB-1::YFP in areas near the nerve ring where ADL and AVA connect each other (White *et al.*, 1986). We found that, in wild-type animals, the expression of SNB-1::YFP was detected in the processes of the ADL neurons close to the nerve ring regions (Figs 3A and B, and EV2A and B). However, the fluorescence level of SNB-1::YFP was significantly decreased in *daf-2* mutants (Figs 3A and B, and EV2A and B). We also monitored the expression of RAB-3 Ras GTPase protein, which plays key roles in synaptic vesicle release (Nonet *et al.*, 1997). In wild-type animals, RAB-3 proteins were consistently detected in the soma and processes of the ADL neurons (Figs 3A and C, and EV2C). Similar to SNB-1, the mCherry-tagged RAB-3 level in ADL was also decreased in both the soma and the processes of *daf-2* mutants (Figs 3A and C, and EV2C). The promoter activity of the *sre-1* gene was not affected by *daf-2* mutations and starvation (Fig EV2D and E; Gruner *et al.*, 2014). We further examined the fluorescence level of OCR-2::mCherry in *daf-2* mutants. *ocr-2* encodes a TRPV channel that acts in the ADL neurons to mediate *ascr#3* avoidance (Jang *et al.*, 2012). We found

that OCR-2 level was not altered in *daf-2* mutants (Fig EV2F). These results suggest that DAF-2 specifically regulates the protein levels of pre-synaptic proteins in the ADL neurons, and then, the reduction in these protein levels in *daf-2* mutants leads to the lack of AVA neuronal responses which eventually result in the suppression of the pheromone avoidance behaviors upon *ascr#3* exposure.

We then examined the SNB-1::YFP level in starved wild-type animals and found that the SNB-1 level was increased in ADL after 6- and 24-h starvation (Fig 3D). Moreover, *daf-2* mutation also suppressed the increase in SNB-1 level in starved wild-type animals (Fig 3E). Together, these results indicate that starvation status may regulate ADL synaptic transmission via the expression levels of synaptic vesicle molecules.

Chemical synaptic outputs of ADL mediate avoidance behaviors to *ascr#3* (Jang *et al.*, 2012; Hong *et al.*, 2017). Consistent with the previous report, blocking of chemical synaptic transmission from ADL by expressing tetanus toxin light chain (TeTx) decreased *ascr#3* avoidance in wild-type animals which appeared not to be further decreased by *daf-2* mutation (Fig 3F; Jang *et al.*, 2012). We next increased the chemical synaptic output of ADL by expressing gain-of-function mutation of *pkc-1* protein kinase C gene which promotes synaptic vesicle fusion (Sieburth *et al.*, 2007; Tsunozaki *et al.*, 2008). We found that the expression of *pkc-1(gf)* enhanced avoidance behavior to *ascr#3* in wild-type animals (Fig 3F). The *daf-2* mutant animals expressing *sre-1p::pkc-1(gf)* also suppressed the enhancement of *ascr#3* avoidance (Fig 3F). These results support that DAF-2 signaling regulates *ascr#3* avoidance by modulating the synaptic activity in ADL. Taken together, these results indicate that feeding status and DAF-2 insulin signaling may regulate ADL synaptic transmission via the change in synaptic vesicle protein levels.

### PI3K/AKT/FOXO act downstream of DAF-2 in ADL to regulate *ascr#3* avoidance behavior

In canonical insulin signaling, DAF-2 signals through AGE-1 (phosphoinositide 3-kinase), PDK-1 (phosphoinositide-dependent kinase), AKT-1/AKT-2 (Akt/protein kinase B family), DAF-18 (PTEN), and DAF-16/FOXO (Kimura *et al.*, 1997; Ogg & Ruvkun, 1998; Engelman *et al.*, 2006; Murphy & Hu, 2013). We investigated whether these genes affect DAF-2-mediate *ascr#3* avoidance behaviors as well as protein levels of SNB-1 in ADL. Similar to *daf-2* mutants, *age-1* or *akt-1* mutants exhibited decreased avoidance to *ascr#3* and SNB-1 level in ADL (Fig 4A and B). However, the mutations in *akt-2*, *pdk-1*, or *daf-18* did not affect *ascr#3* avoidance (Fig 4A).

We next tested *daf-16*, a major downstream target of *daf-2*, and found that the mutation of *daf-16* increased *ascr#3* avoidance behavior under well-fed conditions (Figs 4C and D, and EV3A). Furthermore, we found that this increased *ascr#3* avoidance in *daf-16* mutants was maintained under starved conditions (Fig EV3A). SNB-1 level in ADL was increased in *daf-16* mutants (Fig 4B), and *daf-16;daf-2* double mutants showed increased *ascr#3* avoidance and SNB-1 level similar to that seen in *daf-16* mutants (Fig 4B and D). The expression of *daf-16* cDNA isoform(a) in ADL rescued the *ascr#3* avoidance and SNB-1 level phenotypes of *daf-16* mutants (Fig 4B and E). These results indicate that *daf-16* antagonizes *daf-2* function cell autonomously in ADL to regulate *ascr#3* avoidance and the expression of ADL synaptic proteins. However, *ascr#3* avoidance

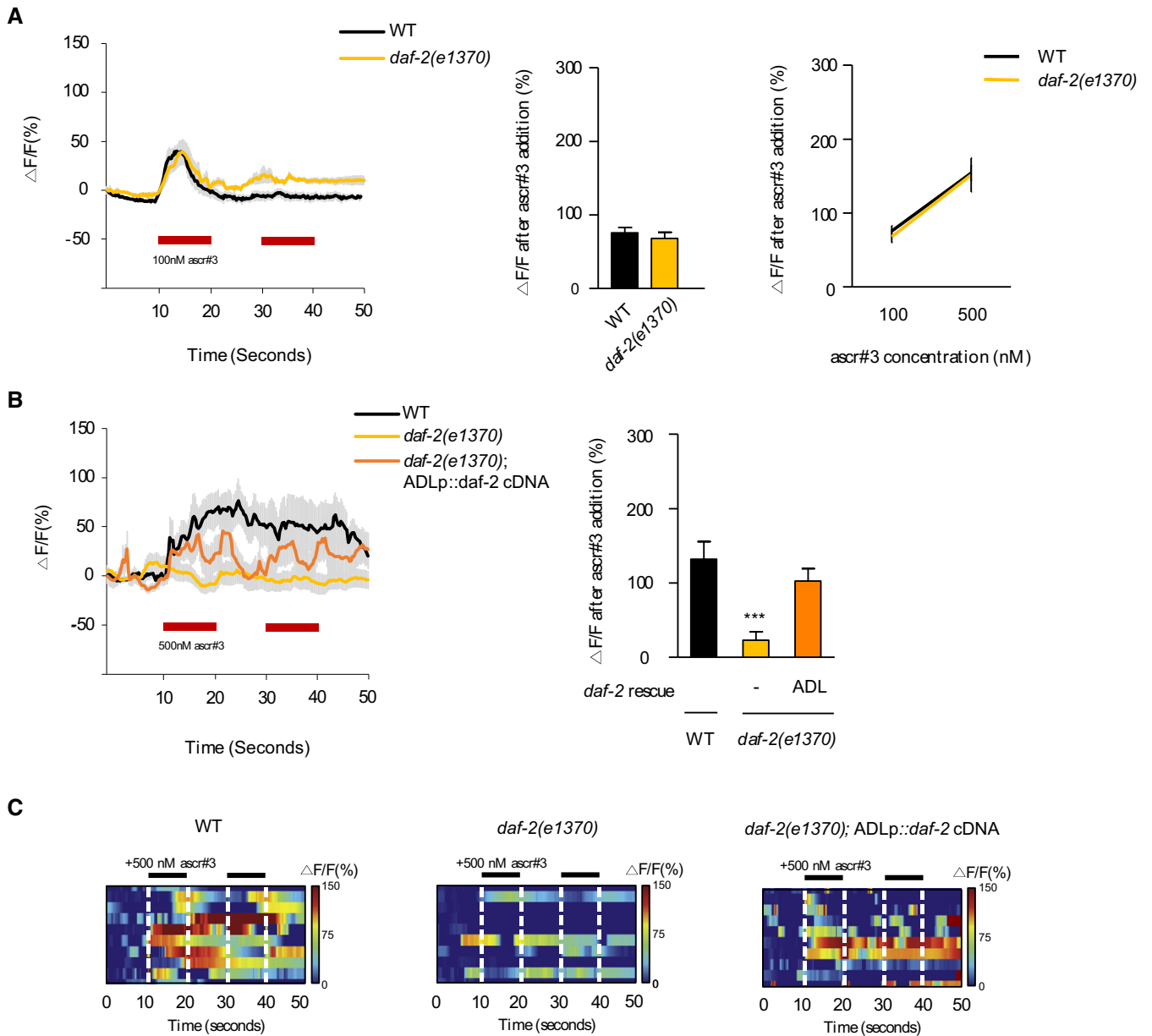


**Figure 2. DAF-2 affects  $Ca^{2+}$  transients not in the ADL ascr#3-sensing neurons but their downstream target neurons.**

A  $Ca^{2+}$  transients of ADL upon ascr#3 exposure in wild-type animals and *daf-2* mutants.  $Ca^{2+}$  transients to 100 nM ascr#3 of ADL (left), the average peak percentage changes in fluorescence upon 100 nM ascr#3 exposure (middle), and the dose–response curve of the average peak percentage changes in fluorescence  $Ca^{2+}$  peaks upon 100 and 500 nM ascr#3 exposure (right).  $n = 7–12$ .

B  $Ca^{2+}$  transients of AVA upon 500 nM ascr#3 exposure in wild-type animals, *daf-2* mutants, and *daf-2* mutants expressing *sre-1p::daf-2* cDNA (ADL).  $Ca^{2+}$  transients in response to ascr#3 in AVA upon 500 nM ascr#3 exposure in wild-type animals (left), the average peak percentage changes in fluorescence upon 100 nM ascr#3 exposure (right).  $n = 10$ .  $***P < 0.001$  (Dunnett’s test).

C Heat-map images of  $Ca^{2+}$  transients in AVA upon 500 nM ascr#3 exposure in wild-type animals (left), *daf-2* mutants (middle), and *daf-2* mutants expressing *sre-1p::daf-2* cDNA (right). Each row represents  $Ca^{2+}$  responses of individual animals to ascr#3 exposure.  $n = 10$ .

Data information: All error bars represent  $\pm$  SEM.

was unaltered in the mutants of a NRF transcription factor/*skn-1*, which is another downstream factor to *daf-2* (Fig EV3B; Ewald et al, 2015), suggesting a specific role of *daf-16* in *daf-2*-mediated ascr#3 avoidance. Taken together, these results further suggest that the DAF-2/AGE-1/AKT-1/DAF-16 signaling pathway mediates feeding state-dependent modulation of ascr#3 avoidance by regulating synaptic outputs of ADL.

**Intestinal INS-18 insulin-like peptide modulates ascr#3 avoidance behavior by inhibiting DAF-2 signaling in ADL**

Next, we sought to identify how feeding status regulates DAF-2 signaling in the ADL sensory neurons. We first searched for ligands for DAF-2 insulin-like receptor by screening a subset of insulin-like peptide (ILPs) mutants including *ins-1*, *ins-7*, *ins-18*, *ins-22*, *ins-32*,

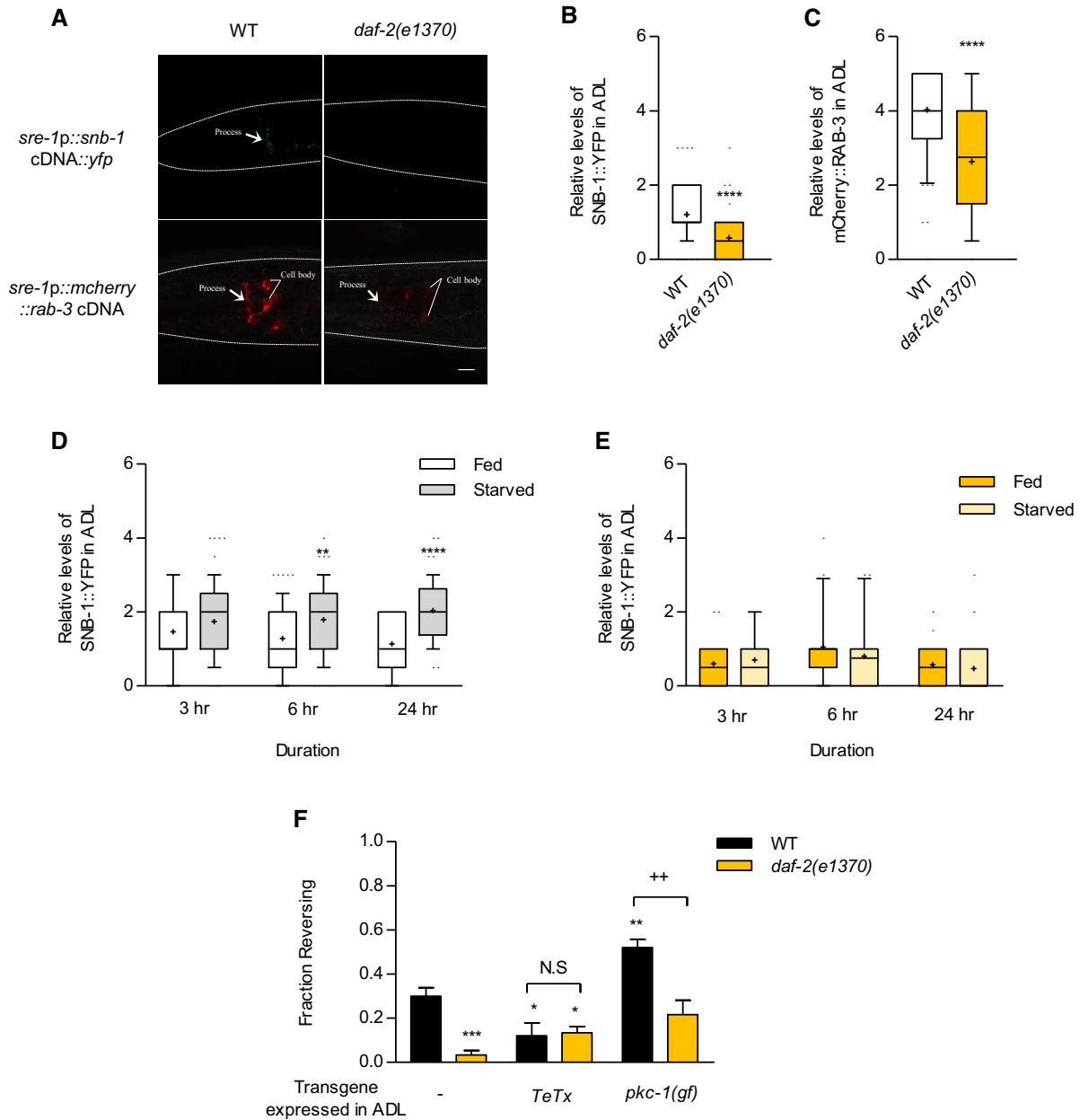


**Figure 3. DAF-2 regulates synaptic transmissions in ADL.**

A Representative images of wild-type animals (left) and *daf-2* mutants (right) expressing *sre-1p::snb-1 cDNA::yfp* (top) and *sre-1p::mCherry::rab-3 cDNA* (bottom). The scale bar is 10  $\mu$ m.

B, C Relative fluorescence intensity of wild-type animals and *daf-2* mutant animals expressing *sre-1p::snb-1 cDNA::yfp* (B) and *sre-1p::mCherry::rab-3 cDNA* (C).  $n = 59-60$ . \*\*\*\* $P < 0.0001$  (unpaired Student's *t*-test).

D Relative fluorescence intensity of *sre-1p::snb-1 cDNA::yfp* of wild-type animals in fed and starved conditions for 3, 6, and 24 h.  $n = 37-80$ . \*\* $P < 0.01$  and \*\*\*\* $P < 0.0001$  (Bonferroni's test).

E Relative fluorescence intensity of *sre-1p::snb-1 cDNA::yfp* of *daf-2* mutants in fed and starved conditions.  $n = 20-30$ .

F Fraction reversing of wild-type animals and *daf-2* mutant animals expressing *sre-1p::TeTx* and *sre-1p::pkc-1(gf)*.  $n = 50-90$ . \* $P < 0.05$ , \*\* $P < 0.01$ , and \*\*\*\* $P < 0.001$  (Dunnnett's test). \*\* $P < 0.01$  (unpaired Student's *t*-test).

Data information: All error bars represent  $\pm$  SEM. Tops and bottoms of boxes indicate the 25<sup>th</sup> and 75<sup>th</sup> percentiles, respectively; whiskers represent 10<sup>th</sup>-90<sup>th</sup> percentile. Median is indicated by a horizontal line and the average is marked by "+" in the box.

*ins-35*, and *daf-28* in well-fed conditions. We found that *ins-1* and *ins-18* mutants showed decreased and increased *ascr#3* avoidance, respectively, but other mutants did not exhibit altered *ascr#3*

avoidance (Fig 5A). We then generated *daf-16;ins-1* double mutants and found that these double mutants showed decreased *ascr#3* avoidance, comparable to that of *ins-1* mutants (Fig 5B), indicating



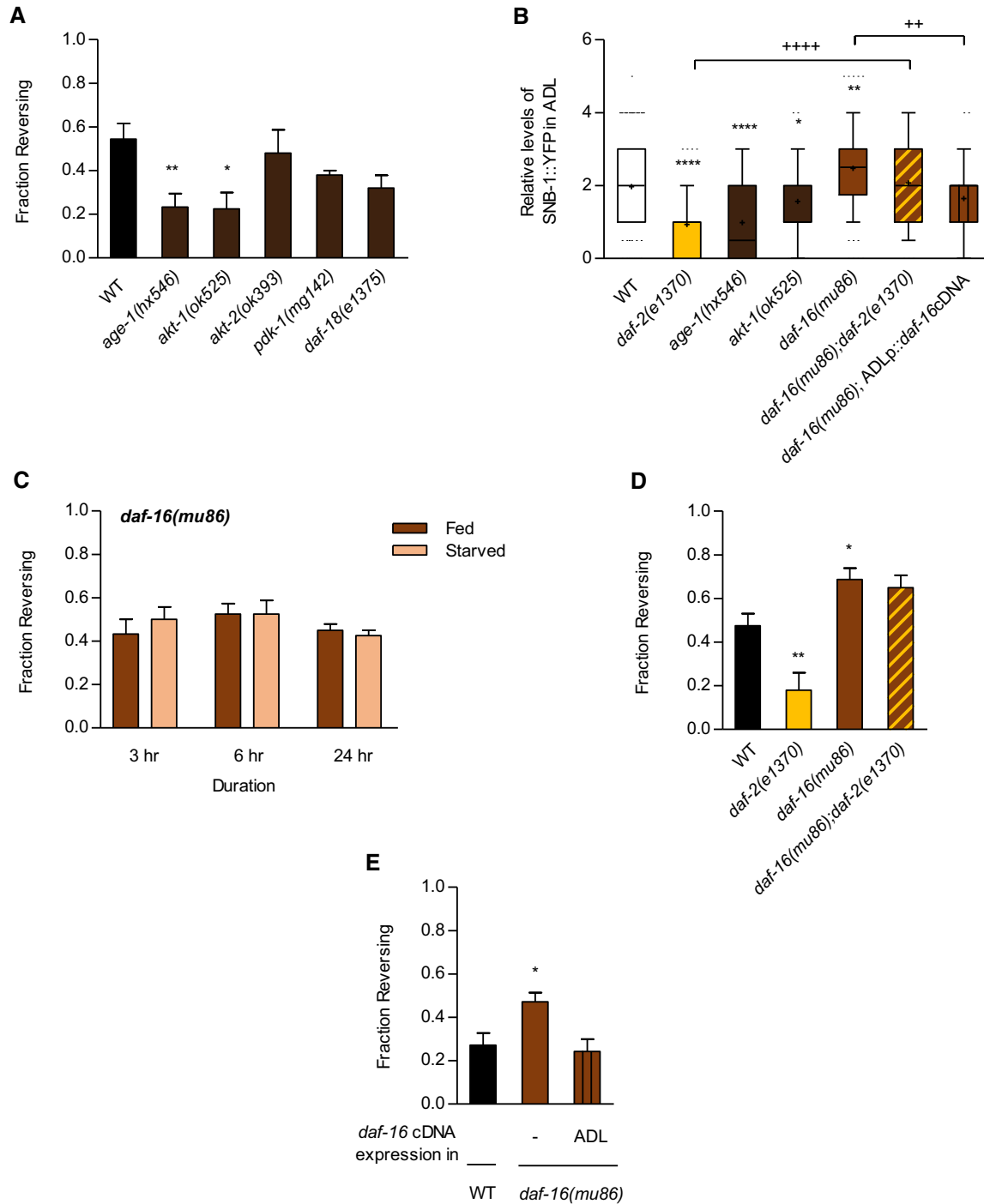


**Figure 4. PI3K/AKT/FOXO pathway acts downstream of *daf-2* signaling in ADL to mediate *ascr#3* avoidance.**

**A** Fraction reversing of wild-type animals, *age-1* mutants, *akt-1* mutants, *akt-2* mutants, and *pdk-1* mutants in response to 500 nM *ascr#3*.  $n = 40-90$ . \* $P < 0.05$  and \*\* $P < 0.01$  (Dunnett's test).

**B** Relative fluorescence intensity of transgenic animals expressing *sre-1p::snb-1 cDNA::yfp*, including *daf-2* mutants, *age-1* mutants, *akt-1* mutants, *daf-16* mutants, *daf-16;daf-2* double mutants, and *daf-16* mutants expressing *sre-1p::daf-16 cDNA* (ADL).  $n = 37-218$ . \*, \*\*, and \*\*\*\* present different from wild type at  $P < 0.05$ ,  $P = 0.01$ , and  $P < 0.0001$  (Dunnett's test). \*\* $P < 0.01$  and \*\*\*\* $P < 0.0001$  (unpaired Student's *t*-test). Tops and bottoms of boxes indicate the 25<sup>th</sup> and 75<sup>th</sup> percentiles, respectively; whiskers represent 10<sup>th</sup>-90<sup>th</sup> percentile. Median is indicated by a horizontal line, and the average is marked by "+" in the box.

**C** Fraction reversing of *daf-16* mutant animals in fed and starved conditions in response to *ascr#3* exposure.  $n = 30-40$ .

**D** Fraction reversing of wild-type animals, *daf-2* mutants, *daf-16* mutants, and *daf-16;daf-2* double mutants in response to *ascr#3*.  $n = 50-80$ . \* $P < 0.05$  and \*\* $P < 0.01$  (Dunnett's test).

**E** Fraction reversing of wild-type animals, *daf-16* mutants, and *daf-16* mutants expressing *sre-1p::daf-16 cDNA* (ADL).  $n = 70$ . \* $P < 0.05$  (Dunnett's test).

Data information: All error bars represent  $\pm$  SEM.

that *ins-1* may function in parallel to or downstream of *daf-2/daf-16* to regulate *ascr#3* avoidance. We next tested *daf-2;ins-18* double mutants and found that *daf-2* mutation suppressed the increase of *ascr#3* avoidance in *ins-18* mutants (Fig 5C). In addition, *ins-18* mutants showed increased SNB-1 level in ADL, and *daf-2* mutation abolished increased SNB-1 level in *ins-18* mutants (Fig 5D and E). These results suggest that INS-18 acts upstream of DAF-2 signaling and that INS-18 antagonizes the DAF-2 function.

Previously, the *ins-18* gene has been shown to be expressed in the neurons and intestine of *C. elegans* (Pierce et al, 2001; Matsunaga et al, 2012; Ritter et al, 2013; Hung et al, 2014). To identify the sites of action of *ins-18*, we expressed *ins-18* cDNA under the pan-neural *unc-14* or *rgef-1* promoter and the intestinal *acd-5* promoter in *ins-18* mutants (Fig EV4A). The *unc-14*, *rgef-1*, and *acd-5* genes encode a RUN domain-containing protein, a Ras guanine nucleotide releasing protein, and an ortholog of the human sodium channels epithelial gene, respectively (Ogura et al, 1997; Altun-Gultekin et al, 2001; Camon et al, 2003). Interestingly, we found that intestinal expression, but not neuronal expression of *ins-18* cDNA fully restored *ascr#3* avoidance and SNB-1 level in *ins-18* mutants (Figs 5E and F, and EV4B), suggesting that the *ins-18* gene expressed in the intestine regulates *ascr#3* avoidance by antagonizing DAF-2 signaling in ADL.

### Feeding state regulates secretion of intestinal INS-18

Since intestinal INS-18 non-cell autonomously modulates the DAF-2/DAF-16 pathway in ADL, we wondered if intestinal *ins-18* expression could be changed by feeding state. However, as previously reported, *ins-18* expression in the intestine, which was monitored by the expression of *ins-18p::gfp* transgene, was unaltered upon starvation (Fig EV5A; Ritter et al, 2013). We next examined whether INS-18 is released from the intestine under fed and starved conditions by measuring GFP accumulation in coelomocytes of transgenic animals expressing functional *acd-5p::ins-18* cDNA::gfp (Hung et al, 2014). Coelomocytes are scavenger cells that uptake secreted proteins into body cavity, and thus, secreted proteins such as ILPs appear to be accumulated in coelomocytes (Fares & Greenwald, 2001; Sieburth et al, 2007). We found that INS-18::GFP was consistently accumulated in fed animals (Fig 6A and B). However, INS-18::GFP accumulation was gradually decreased from 1 to 24 h of starvation (Fig 6A and B). Moreover, this decreased INS-18 secretion was restored by 24 h of re-feeding

(Fig 6C), suggesting that feeding state regulates the secretion of intestinal INS-18. To further investigate the roles of INS-18 secretion on the modulation of DAF-2 pathway in ADL, we temporarily knocked down *ins-18* function for 6 and 24 h using RNA interference (RNAi). Although *ins-18* knockdown for 6 h did not alter intestinal INS-18 release which is probably due to insufficient time for RNAi for 6-h mimicking starvation for 6 h (Kamath et al, 2003), *ins-18* knockdown for 24 h decreased intestinal INS-18 release and improved *ascr#3* avoidance, as observed in starved animals (Fig 6D and E). We next knocked down *ins-18* for 24 h in *daf-2* mutant animals. Similar to the effects on *ins-18* mutants, *daf-2* mutation suppressed the increase of *ascr#3* avoidance in *ins-18* RNAi-treated worms, and the expression of *daf-2* cDNA in ADL restored the enhanced *ascr#3* avoidance in *ins-18* RNAi-treated *daf-2* mutants (Fig 6E). In addition, *ins-18* RNAi for 24 h also increased SNB-1 level in ADL (Fig 6F). In summary, these results indicate that temporal regulation of INS-18 secretion from the intestine plays a major role in feeding state-dependent *ascr#3* avoidance mediated by ADL.

## Discussion

In this study, we analyzed the mechanisms underlying the modulation of *ascr#3* avoidance behaviors by feeding status. Our data support a model in which prolonged starvation decreases secretion of INS-18 insulin-like peptide from the intestine, and INS-18 antagonistically acts on DAF-2 insulin-like pathway in *ascr#3*-sensing ADL neurons, which regulate the strength of ADL synaptic outputs and thus *ascr#3* avoidance behaviors (Fig 7). *ascr#3* is the potent aversive pheromone in *C. elegans* hermaphrodites representing harsh conditions of overcrowding (Jang et al, 2012; Hong et al, 2017). Thus, starved animals may enhance avoidance behavior for harsh conditions to find more affordable conditions.

In *Drosophila*, insulin signaling also regulates feeding state-dependent chemosensory responses. For example, flies starved for over 4 h exhibit increased attractive behaviors to food odorants, including vinegar (Root et al, 2011; Ko et al, 2015). These behavioral changes are mediated by increased synaptic activities of vinegar-responsive olfactory sensory neurons (OSNs) to downstream target neurons, which are facilitated by increased expression of the short neuropeptide F receptor sNPF1 in the same OSNs. Starvation appears to decrease circulating insulin level which subsequently

**Figure 5. INS-18, which is secreted in the intestine, inhibits DAF-2 signaling in ADL.**

- A Fraction reversing of insulin-like peptide mutants, *ins-1*, *ins-7*, *ins-18*, *ins-22*, *ins-32*, *ins-35*, and *daf-28* in response to *ascr#3*.  $n = 40\text{--}170$ . \* $P < 0.05$  and \*\*\* $P < 0.001$  (Dunnett's test).
- B Fraction reversing of wild-type animals, *ins-1* mutants, *daf-16* mutants, and *daf-16;ins-1* double mutants in response to *ascr#3*.  $n = 60\text{--}70$ . \* $P < 0.05$  (Dunnett's test).
- C Fraction reversing of wild-type animals, *daf-2* mutants, *ins-18* mutants, and *daf-2;ins-18* double mutants in response to *ascr#3*.  $n = 70$ . \* $P < 0.05$  and \*\*\* $P < 0.01$  (Dunnett's test).
- D Representative images of wild-type animals (right) and *ins-18* mutants (left) expressing *sre-1p::snb-1* cDNA::yfp. Scale bar is 10  $\mu\text{m}$ .
- E Relative fluorescence intensity of *sre-1p::snb-1* cDNA::yfp in wild-type animals, *daf-2* mutants, *ins-18* mutants, *daf-2;ins-18* double mutants, and *ins-18* mutants expressing *unc-14p::ins-18* cDNA (neuron) and *acd-5p::ins-18* cDNA (intestine).  $n = 35\text{--}75$ . \*\*\*\* $P < 0.0001$  (Dunnett's test). \*\*\*\* $P < 0.0001$  (unpaired Student's test). Tops and bottoms of boxes indicate the 25<sup>th</sup> and 75<sup>th</sup> percentiles, respectively; whiskers represent 10<sup>th</sup>–90<sup>th</sup> percentile. Median is indicated by a horizontal line, and the average is marked by "+" in the box.
- F Fraction reversing of wild-type animals, *ins-18* mutants, and *ins-18* mutants expressing *unc-14p::ins-18* cDNA (neuron), and *ins-18* mutants expressing *acd-5p::ins-18* cDNA (intestine).  $n = 60$ . \* $P < 0.05$  (Dunnett's test). \*\*\* $P < 0.001$  (unpaired Student's test).

Data information: All error bars represent  $\pm$  SEM.



increases sNPF1 expression via insulin receptor activity in OSNs, causing enhanced synaptic transmission of OSNs and the consequent attraction behaviors (Root et al, 2011). Thus, these basic endocrine and circuit mechanisms underlying prolonged

starvation-induced behavioral changes in *Drosophila* are comparable to those identified by us in *C. elegans*, suggesting an evolutionarily conserved mechanisms underlying feeding state-dependent behavioral plasticity.

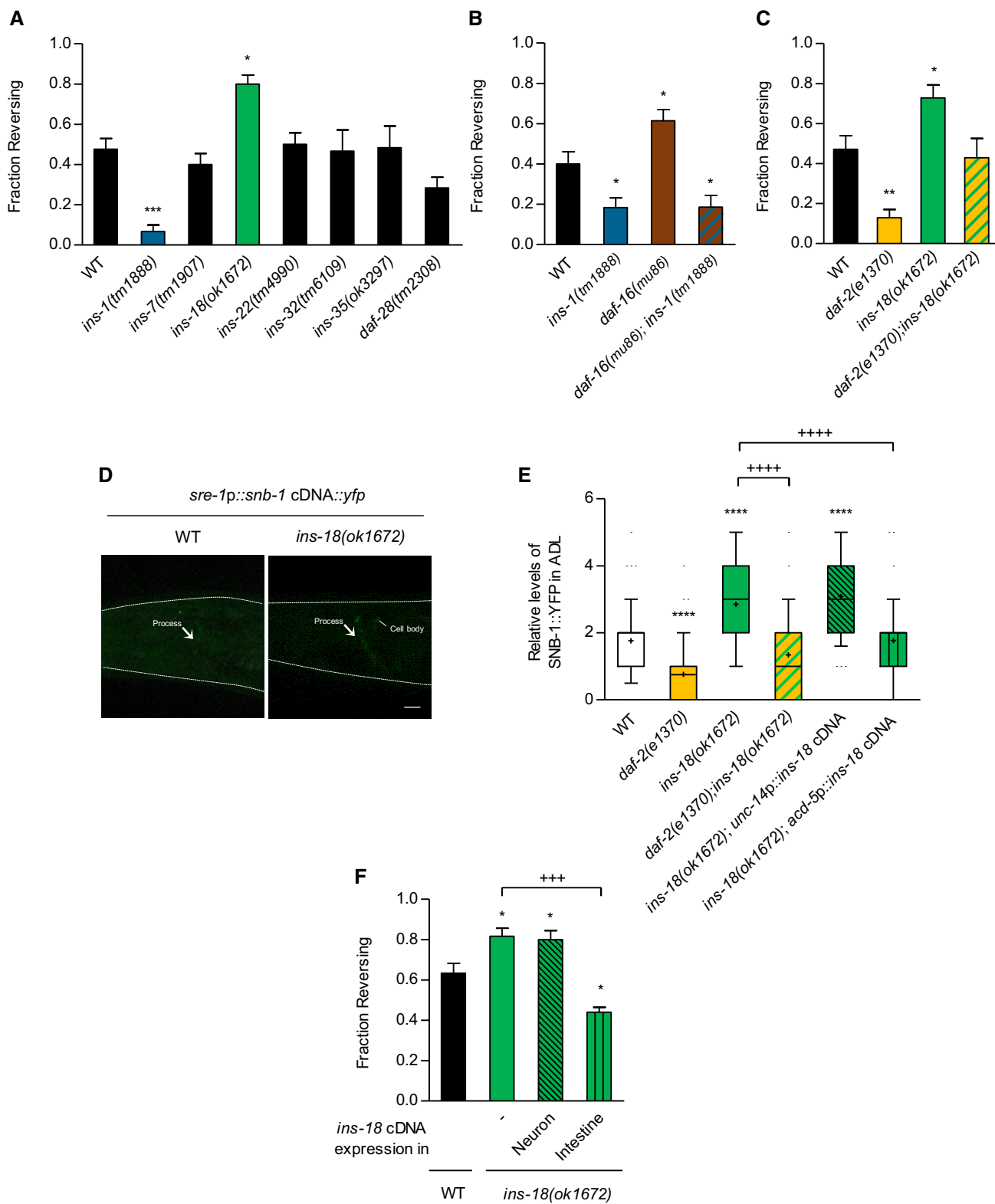
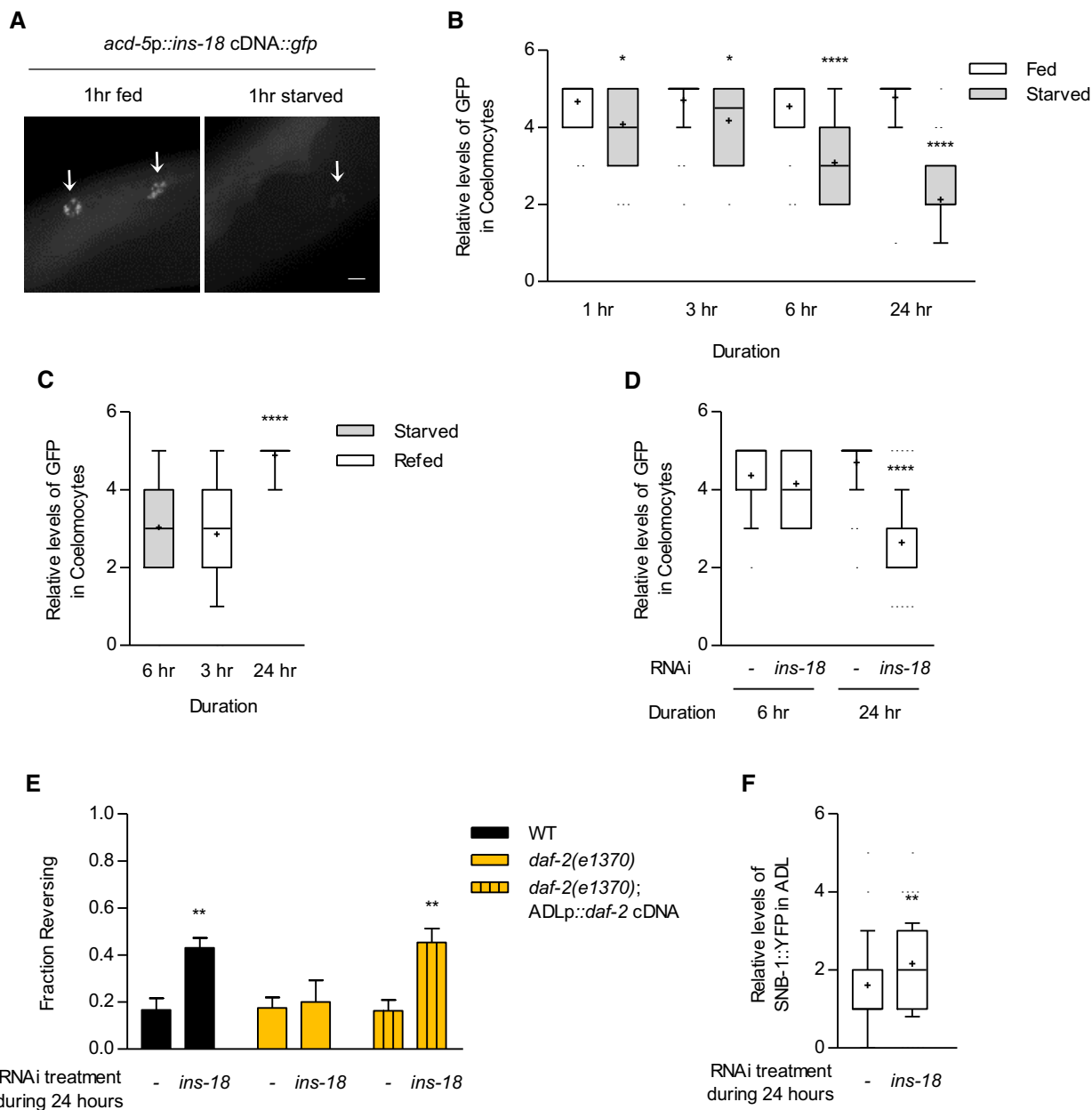


Figure 5.



**Figure 6. Intestinal INS-18 secretion modulates ascr#3 avoidance in a feeding state-dependent fashion.**

A Representative images of transgenic animals expressing *acd-5p::ins-18 cDNA::gfp* at 1-h fed and starved conditions. Arrows indicate coelomocyte. Scale bar is 10  $\mu$ m.

B, C Relative fluorescence intensity of the accumulated GFP of transgenic animals expressing *acd-5p::ins-18 cDNA::gfp* in coelomocytes at different times after feeding, starving (B), and re-feeding conditions (C).  $n = 39-50$ . (B)  $*P = 0.05$  and  $****P < 0.0001$  (Bonferroni's test). (C)  $****P < 0.0001$  (Dunnett's test).

D Relative fluorescence intensity of the accumulated GFP of transgenic animals expressing *acd-5p::ins-18 cDNA::gfp* in coelomocytes under *ins-18* RNAi treatment.  $n = 36-59$ .  $****P < 0.0001$  (Bonferroni's test).

E Fraction reversing of wild-type animals, *daf-2* mutants, and *daf-2* mutants expressing *sre-1p::daf-2 cDNA* treated with *ins-18* RNAi for 24 h.  $n = 80-100$ .  $**P < 0.01$  (Bonferroni's test).

F Relative fluorescence intensity of wild-type animals expressing *sre-1p::snb-1 cDNA::yfp* in 24 h-*ins-18* RNAi condition.  $n = 57-58$ .  $**P < 0.01$  (unpaired Student's t-test).

Data information: All error bars represent  $\pm$  SEM. Tops and bottoms of boxes indicate the 25<sup>th</sup> and 75<sup>th</sup> percentiles, respectively; whiskers represent 10<sup>th</sup>-90<sup>th</sup> percentile. Median is indicated by a horizontal line, and the average is marked by "+" in the box.

It was previously shown that an insulin-like peptide, INS-1, regulates food-related odor responses in *C. elegans* (Chalasan *et al*, 2010). In *ins-1* mutants,  $Ca^{2+}$  activities of the AWC olfactory

neurons in response to food-related odorants are increased, and thus, AWC-mediated behaviors are enhanced, suggesting that similar to negative regulatory role of INS-18 in the ADL neuronal

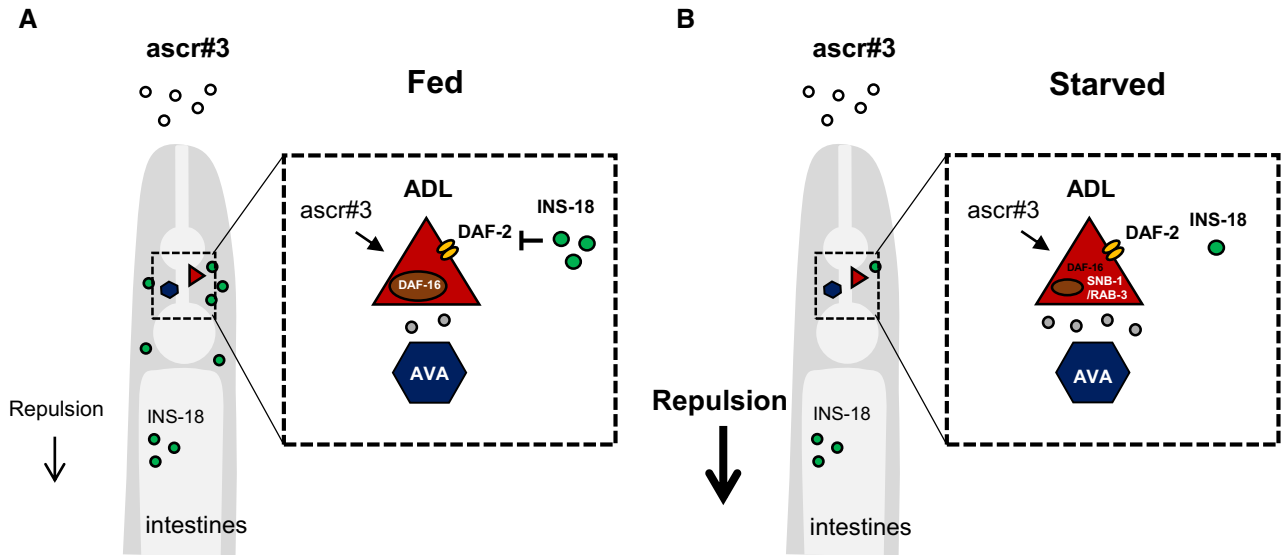


**Figure 7. A model for feeding state-dependent modulation of *ascr#3* avoidance behaviors.**

- A In fed conditions, INS-18 released from the intestine blocks the activity of DAF-2 signaling in ADL, which suppresses chemical synaptic transmission in ADL and decreases avoidance behavior to *ascr#3*.
- B In starved conditions, secretion of INS-18 from the intestine is decreased, which activates the DAF-2 signaling of ADL, resulting in increase in synaptic release from ADL to downstream neurons, and promotes enhanced avoidance behavior to *ascr#3*.

activities found in our study, INS-1 dampens the activities of the AWC olfactory neurons (Chalasan *et al*, 2010). Here, we also found distinct roles of INS-1 in *ascr#3* avoidance, which is strongly decreased in *ins-1* mutants, suggesting a positive regulatory role of INS-1 in *ascr#3* avoidance behaviors (Fig 5A). Since INS-1 acts in AWC post-synaptic target AIA interneurons to regulate AWC activities in feedback loop, it is intriguing to identify where INS-1 acts and how INS-1 interacts with INS-18 to regulate *ascr#3* avoidance.

Park *et al* (2017) showed that *C. elegans* hermaphrodites avoid high concentration of *ascr#1* (daumone-1) and *ascr#2*, in addition to *ascr#3*. Moreover, avoidance to these three pheromones is decreased in *daf-16* mutants but not altered in *daf-2* mutants, which is different from what we found in this study: *ascr#3* avoidance is increased in *daf-16* mutants of which mutations suppressed decreased *ascr#3* avoidance in *daf-2* mutants. In addition, we and other laboratories have not observed *ascr#2* avoidance (Jang *et al*, 2012; Hong *et al*, 2017). This discrepancy could be due to different assay systems used in these studies; we performed the drop assay with a single animal, whereas Park *et al* mainly used the classic chemotaxis assay with population animals. The drop assay detects acute avoidance within 1 s upon direct pheromone exposure to animals, whereas classic population assay determines stationary response to the concentration gradient of a chemical in an hour; thus, the results from these assays may reflect different aspects of avoidance responses to pheromones (Bargmann *et al*, 1993; Jang & Bargmann, 2013). Other possibilities are different genetic backgrounds of wild-type and mutant animals and/or quality and quantity of reagents, including pheromones, used (Lucanic *et al*, 2017). It would be intriguing to explore this problem in the future.

Previously, Gruner *et al* (2014, 2016) showed that the expression of the ADL-specific chemoreceptor gene, *srh-234*, is also

regulated by the feeding state of an animal and insulin signaling. Prolonged starvation causes downregulation of the *srh-234* gene expression, which appears to be mediated by *daf-2* in the *daf-16*-dependent manner acting in ADL. Compared to our studies wherein prolonged starvation increased *daf-2* signaling in the ADL neurons to increase *ascr#3* avoidance behavior, the starvation condition decreased *daf-2* signaling in the ADL neurons to decrease *srh-234* expression (Gruner *et al*, 2014). In addition, mutually exclusive sets of insulin-like peptides, most of which seem to be secreted from the intestine, are involved: INS-18 and INS-1 for *ascr#3* avoidance and INS-3, INS-7, INS-21, INS-26, and INS-28 for the *srh-234* gene expression in the ADL neurons (Gruner *et al*, 2016). Moreover, *srh-234* expression is further regulated by multiple signaling pathways, including the NPR-1 neuropeptide, KIN-29 salt-inducible kinase, and OCR-2 TRPV channels, as well as the presence of food (Gruner *et al*, 2014). Moreover, the expression of another ADL-expressed gene, *srh-34*, is upregulated by starvation (Gruner *et al*, 2014). Therefore, their results together with our results suggest a multitude of complexity in the function of and/or gene expression in the ADL sensory neurons. Investigating *ascr#3* avoidance behaviors in other internal and external contexts and identifying *srh-234* gene function would be the next step to address different roles of insulin signaling in between *ascr#3* avoidance and *srh-234* gene expression.

Neuromodulatory systems in the intestine-sensory neuron axis play key roles to integrate feeding state with external environmental cues and shape the activities of peripheral as well as central system to generate appropriate behavioral outcomes. Our study showed that systemic circuit mechanisms underlie feeding state-dependent modulation of synaptic activities at the sensory level and suggest *C. elegans* as a good model system to further study this type of behavioral plasticity.

## Materials and Methods

### Strains and constructs

N2 strain was used as the wild-type animals. All strains were maintained on *Escherichia coli* OP50-seeded NGM plates at 20°C (Brenner, 1974). The strains used in this study are listed in Table EV1.

pJH664 (*rgef-1p::daf-2* cDNA), pVDL14 (*sre-1p::daf-2* cDNA, SL2::*mCherry*), and pMG14 (*sre-1p::daf-16a* cDNA, SL2::*mCherry*), which were kind gifts from Mei Zhen and Alexander van der Linden, were used for *daf-2* and *daf-16* rescue in pan-neuronal and ADL experiments. *ins-18* cDNA was amplified and inserted into pMC10 vector using the restriction enzymes *AgeI* and *NotI*, and the promoter region of *unc-14* or *acd-5* was placed into the plasmids using the each pairs of enzymes—*HindIII* and *BamHI* or *SphI* and *XmaI* for *ins-18* cDNA expression in neuron and the intestine, respectively.

*sre-1p::mCherry::rab-3* cDNA was prepared by exchanging the promoter region of MVC016 (*nlp::mCherry::rab-3* cDNA, a kind gift from Miri VanHoven) via restriction enzyme sites of *SphI* and *SmaI*, and *sre-1p::snb-1* cDNA::*yfp* were constructed from PCZ530 (*unc-25p::snb-1* cDNA::*yfp*, a kind gift from Yishi Jin).

*sre-1p::gfp* and *sre-1p::mCherry* transgenes were produced by cutting the *sre-1* promoter from *sre-1p::GCaMP3* and subcloning into pPD95.77 or MC10 vector which contains *gfp* and *mCherry* through enzyme target sites *HindIII* and *BamHI*.

*ins-18* cDNA::*gfp* was extracted from pJH1498 (*su006p::ins-18* cDNA::*gfp*, a kind gift by Mei Zhen) and was attached to *acd-5* promoter in MC10 vector.

All plasmids were injected at 5–15 ng (rescue experiments) and 50 ng (expression analysis) with *unc-122p::gfp* or *unc-122p::dsRed*, which were injection markers.

### ascr#3 avoidance assay

ascr#3 avoidance assay was modified from a previously described drop assay (Jang *et al*, 2012; Hong *et al*, 2017). All assays were performed in the absence of food at 20°C. We usually used 500 nM ascr#3, which was diluted into M13 buffer, in the assay, except under the conditions of Fig 1B–D and G, and EV1D wherein 100 nM ascr#3 was applied, and those of Figs 1E and EV3A and B, wherein 100, 200, and 400 nM ascr#3 were applied (detailed ascr#3 concentration was noted in figure legends). In the assay, young adult animals were transformed onto non-seeded plates. M13 buffer was delivered on the tip of the head, and if the animals did not response to M13 buffer for 10 s, we dropped ascr#3 on the freely moving animal's head. Short or long reversals were defined as reversals with fewer than two head bends or more than two head bends, respectively. Long reversal responding to ascr#3 within 4 s was counted as an avoidance behavior.

### Starvation assay

The starvation assay was based on a previously described method (Gruner *et al*, 2014). Ten young adults were placed on an OP50 seeded plate for egg laying and discarded in 2–4 h to synchronize animal stage. The animals were grown at 20°C for about 3 days, washed with distilled water, and placed onto seeded or non-seeded plates for 3, 6, and 24 h. For re-feeding OP50, animals starved for

6 h were transferred onto a seeded plate, and ascr#3 avoidance was tested for 3, 6, and 24 h, respectively.

### In vivo Ca<sup>2+</sup> imaging

We followed a previously published *in vivo* Ca<sup>2+</sup> imaging protocol (Jang *et al*, 2012). Custom-made microfluidic chips were processed as previously described (Chronis *et al*, 2007). GCaMP3 attached with the promoter of *sre-1* and *nmr-1* was utilized for ADL and AVA imaging, respectively. In the imaging processes, the transgenic animals were exposed to fluorescence light for 1–2 min, and the images were taken during 1 min under fixed exposure time using 40× objective of a Zeiss Axioplan microscope with a Zeiss AxioCam HR. We used Image J and custom-written MATLAB to analyze the acquired images. More specifically, the cell body area of an ADL neuron was selected as the region of interest and a similar sized area near the cell body was selected as the background. Average fluorescence intensities in the first 5 s of imaging were used for normalization to calculate  $\Delta F/F$ . The peak of “ $\Delta F/F$ ” represented maximum  $\Delta F/F$  during the first ascr#3 exposure, and these data were averaged to obtain the average peak of  $\Delta F/F$ .

### Fluorescence quantification

The expression of *sre-1p::gfp* and *sre-1p::mCherry* was measured by grading the fluorescence brightness from 0 to 5 (as assessed by the naked eye), in the increasing order, following expressions in cell body and processes of ADL. For example, strongly bright fluorescence in both the soma and processes was ranked as 4 or 5. The expression without GFP reflection in the soma and processes was graded as 3. Weak expression in the soma but not in the process was ranked as 1 or 2.

The intensity of *snb-1* cDNA and *rab-3* cDNA in ADL was examined by monitoring the expression of puncta in ADL processes located in the middle of the nerve ring where ADL has synaptic connections to AVA (White *et al*, 1986). When SNB-1 or RAB-3 proteins were localized in both the soma and processes (Fig 3A: RAB-3 expression in wild-type animals), we counted the brightness as 4 or 5. Brightness was ranked as 3 for visual fluorescence expression in ADL processes but not in the soma. Brightness level 1 and 2 represented faint or dim fluorescent expression in the middle of the process in ADL.

To quantify expression levels of SNB-1::YFP and mCherry::RAB-3 represented in Fig EV2B and C, we captured images of *sre-1p::snb-1* cDNA::*yfp* and *sre-1p::mCherry::rab-3* cDNA expression in the ADL neurons with a Zeiss Axioplan microscope using a 40× objective and a CCD camera (Hamamatsu). Then, we measured fluorescence levels using Image J software (<https://imagej.nih.gov/ij/index.html>).

The quantifications of the expressions of *sre-1p::gfp*, *sre-1p::mCherry*, *sre-1p::snb-1* cDNA::*yfp*, *sre-1p::mCherry::rab-3* cDNA, and *acd-5p::gfp::ins-18* cDNA were performed under a 40× objective lens of Zeiss Axioplan microscopy, except for the images of *acd-5p::gfp*, which were acquired under a 10× objective lens.

The representative images were obtained using Zeiss LSM700/780 confocal microscope and Zeiss Axioplan microscope, and the acquired images were edited using ZEN 2010 light edition software and ImageJ.

### ins-18 RNAi treatment

We followed a previously described RNAi feeding method (Kamath et al, 2003). *ins-18* RNAi was kindly provided by Jeong-Hoon Hahm. NGM plates that contained IPTG were seeded using bacteria HT115 or HT115 containing *ins-18* RNAi grown in LB broth; they were then placed at room temperature for ~2 days in the dark. Young adult animals were placed onto the IPTG plates seeded for 6 and 24 h. Then, we examined rates of SNB-1::YFP in ADL and avoidance behaviors using 500 nM *ascr#3*.

### Statistical analysis

All statistical analyses were performed using the software Prism 5.0/7.0. Difference of two groups of subjects was evaluated using a two-tailed unpaired Student's *t*-test. One-way ANOVA test analyzed more than multiple subjects, such as Dunnett's test (individual comparisons) and Bonferroni's test (paired group comparisons). SEM is indicated by error bars in each graph. More statistical information is represented in all figure legends.

**Expanded View** for this article is available online.

### Acknowledgements

We thank Oliver Hobert, Cornelia Bargmann, Yishi Jin, Alexander van der Linden, and Mei Zhen for reagents and the *Caenorhabditis* Genetics Center (NIH Office of Research Infrastructure Programs, P40 OD010440) and the National BioResource Project (Japan) for strains. We also thank Alexander van der Linden, Jeong-Hoon Hahm, Young-Jae You, Sunkyung Lee, Seung-Jae V. Lee, S.V. Lee laboratory members, and K. Kim laboratory members for helpful comments and discussion on the manuscript. This work was supported by the KBRI Basic Research Program of the Ministry of Science, ICT and Future Planning (17-BR-04), the National Research Foundation of Korea (NRF-2015R1D1A1A09061430, NRF-2017R1A4A1015534), and DGIST R&D Program of the Ministry of Science, ICT and Future Planning (17-BD-06) (K.K.), the KBSI grant (#T37416) (Y.H.H), and NIH GM087533 and GM118775 (R.A.B).

### Author contributions

LR, YJC, and YHH performed the experiments; SP, SC, HC, and RAB provided reagents; LR, YHH, and KK analyzed and interpreted data; and LR and KK wrote the manuscript.

### Conflict of interest

The authors declare that they have no conflict of interest.

## References

- Altun-Gultekin Z, Andachi Y, Tsalik EL, Pilgrim D, Kohara Y, Hobert O (2001) A regulatory cascade of three homeobox genes, *ceh-10*, *ttx-3* and *ceh-23*, controls cell fate specification of a defined interneuron class in *C. elegans*. *Development* 128: 1951–1969
- Avery L, Thomas JH (1997) Feeding and defecation. In *C. elegans* II, Riddle DL, Blumenthal T, Meyer BJ, Priess JR (eds), pp 679–716. Cold Spring Harbor, NY: Cold Spring Harbor Laboratory Press
- Bargmann CI, Hartwig E, Horvitz HR (1993) Odorant-selective genes and neurons mediate olfaction in *C. elegans*. *Cell* 74: 515–527
- Brenner S (1974) The genetics of *Caenorhabditis elegans*. *Genetics* 77: 71–94
- Butcher RA, Fujita M, Schroeder FC, Clardy J (2007) Small-molecule pheromones that control dauer development in *Caenorhabditis elegans*. *Nat Chem Biol* 3: 420–422
- Camon E, Magrane M, Barrell D, Binns D, Fleischmann W, Kersey P, Mulder N, Oinn T, Maslen J, Cox A, Apweiler R (2003) The Gene Ontology Annotation (GOA) project: implementation of GO in SWISS-PROT, TrEMBL, and InterPro. *Genome Res* 13: 662–672
- Chalasan SH, Kato S, Albrecht DR, Nakagawa T, Abbott LF, Bargmann CI (2010) Neuropeptide feedback modifies odor-evoked dynamics in *Caenorhabditis elegans* olfactory neurons. *Nat Neurosci* 13: 615–621
- Chalfie M, Sulston JE, White JG, Southgate E, Thomson JN, Brenner S (1985) The neural circuit for touch sensitivity in *Caenorhabditis elegans*. *J Neurosci* 5: 956–964
- Chronis N, Zimmer M, Bargmann CI (2007) Microfluidics for *in vivo* imaging of neuronal and behavioral activity in *Caenorhabditis elegans*. *Nat Methods* 4: 727–731
- Colbert HA, Bargmann CI (1997) Environmental signals modulate olfactory acuity, discrimination, and memory in *Caenorhabditis elegans*. *Learn Mem* 4: 179–191
- Critchley HD, Rolls ET (1996) Hunger and satiety modify the responses of olfactory and visual neurons in the primate orbitofrontal cortex. *J Neurophysiol* 75: 1673–1686
- Edison AS (2009) *Caenorhabditis elegans* pheromones regulate multiple complex behaviors. *Curr Opin Neurobiol* 19: 378–388
- Engelman JA, Luo J, Cantley LC (2006) The evolution of phosphatidylinositol 3-kinases as regulators of growth and metabolism. *Nat Rev Genet* 7: 606–619
- Ewald CY, Landis JN, Porter Abate J, Murphy CT, Blackwell TK (2015) Dauer-independent insulin/IGF-1-signalling implicates collagen remodelling in longevity. *Nature* 519: 97–101
- Ezurra M, Tanizawa Y, Swoboda P, Schafer WR (2011) Food sensitizes *C. elegans* avoidance behaviours through acute dopamine signalling. *EMBO J* 30: 1110–1122
- Ezurra M, Walker DS, Beets I, Swoboda P, Schafer WR (2016) Neuropeptidergic signaling and active feeding state inhibit nociception in *Caenorhabditis elegans*. *J Neurosci* 36: 3157–3169
- Fadoo DA, Tucker K, Phillips JJ, Simmen JA (2000) Brain insulin receptor causes activity-dependent current suppression in the olfactory bulb through multiple phosphorylation of Kv1.3. *J Neurophysiol* 83: 2332–2348
- Fares H, Greenwald I (2001) Genetic analysis of endocytosis in *Caenorhabditis elegans*: coelomocyte uptake defective mutants. *Genetics* 159: 133–145
- Gruner M, Nelson D, Winbush A, Hintz R, Ryu L, Chung SH, Kim K, Gabel CV, van der Linden AM (2014) Feeding state, insulin and NPR-1 modulate chemoreceptor gene expression via integration of sensory and circuit inputs. *PLoS Genet* 10: e1004707
- Gruner M, Grubbs J, McDonagh A, Valdes D, Winbush A, van der Linden AM (2016) Cell-autonomous and non-cell-autonomous regulation of a feeding state-dependent chemoreceptor gene via MEF-2 and bHLH transcription factors. *PLoS Genet* 12: e1006237
- Hills T, Brockie PJ, Maricq AV (2004) Dopamine and glutamate control area-restricted search behavior in *Caenorhabditis elegans*. *J Neurosci* 24: 1217–1225
- Hong M, Ryu L, Ow MC, Kim J, Je AR, Chinta S, Huh YH, Lee KJ, Butcher RA, Choi H, Sengupta P, Hall SE, Kim K (2017) Early pheromone experience modifies a synaptic activity to influence adult pheromone responses of *C. elegans*. *Curr Biol* 27: 3168–3177
- Hung WL, Wang Y, Chitturi J, Zhen M (2014) A *Caenorhabditis elegans* developmental decision requires insulin signaling-mediated neuron-intestine communication. *Development* 141: 1767–1779
- Jang H, Kim K, Neal SJ, Macosko E, Kim D, Butcher RA, Zeiger DM, Bargmann CI, Sengupta P (2012) Neuromodulatory state and sex specify alternative



- behaviors through antagonistic synaptic pathways in *C. elegans*. *Neuron* 75: 585–592
- Jang H, Bargmann CI (2013) Acute behavioral responses to pheromones in *C. elegans* (adult behaviors: attraction, repulsion). *Methods Mol Biol* 1068: 285–292
- Jeong PY, Jung M, Yim YH, Kim H, Park M, Hong E, Lee W, Kim YH, Kim K, Paik YK (2005) Chemical structure and biological activity of the *Caenorhabditis elegans* dauer-inducing pheromone. *Nature* 433: 541–545
- Kamath RS, Fraser AG, Dong Y, Poulin G, Durbin R, Gotta M, Kanapin A, Le Bot N, Moreno S, Sohrmann M, Welchman DP, Zipperlen P, Ahringer J (2003) Systematic functional analysis of the *Caenorhabditis elegans* genome using RNAi. *Nature* 421: 231–237
- Kimura KD, Tissenbaum HA, Liu Y, Ruvkun G (1997) *daf-2*, an insulin receptor-like gene that regulates longevity and diapause in *Caenorhabditis elegans*. *Science* 277: 942–946
- Ko KI, Root CM, Lindsay SA, Zaninovich OA, Shepherd AK, Wasserman SA, Kim SM, Wang JW (2015) Starvation promotes concerted modulation of appetitive olfactory behavior via parallel neuromodulatory circuits. *eLife* 4: e08298
- Lacroix MC, Badonnel K, Meunier N, Tan F, Schlegel-Le Poupon C, Durieux D, Monnerie R, Baly C, Congar P, Salesses R, Caillol M (2008) Expression of insulin system in the olfactory epithelium: first approaches to its role and regulation. *J Neuroendocrinol* 20: 1176–1190
- Lakowski B, Hekimi S (1998) The genetics of caloric restriction in *Caenorhabditis elegans*. *Proc Natl Acad Sci USA* 95: 13091–13096
- Lemieux GA, Ashrafi K (2015) Neural regulatory pathways of feeding and fat in *Caenorhabditis elegans*. *Annu Rev Genet* 49: 413–438
- Lopez AL, Chen J, Joo HJ, Drake M, Shidate M, Kseib C, Arur S (2013) DAF-2 and ERK couple nutrient availability to meiotic progression during *Caenorhabditis elegans* oogenesis. *Dev Cell* 27: 227–240
- Lucanic M, Plummer WT, Chen E, Harke J, Foulger AC, Onken B, Coleman-Hulbert AL, Dumas KJ, Guo S, Johnson E, Bhaumik D, Xue J, Crist AB, Presley MP, Harinath G, Sedore CA, Chamoli M, Kamat S, Chen MK, Angeli S et al (2017) Impact of genetic background and experimental reproducibility on identifying chemical compounds with robust longevity effects. *Nat Commun* 8: 14256
- Macosko EZ, Pokala N, Feinberg EH, Chalasani SH, Butcher RA, Clardy J, Bargmann CI (2009) A hub-and-spoke circuit drives pheromone attraction and social behaviour in *C. elegans*. *Nature* 458: 1171–1175
- Magni P, Dozio E, Ruscica M, Celotti F, Masini MA, Prato P, Broccoli M, Mambro A, More M, Strollo F (2009) Feeding behavior in mammals including humans. *Ann N Y Acad Sci* 1163: 221–232
- Matsunaga Y, Gengyo-Ando K, Mitani S, Iwasaki T, Kawano T (2012) Physiological function, expression pattern, and transcriptional regulation of a *Caenorhabditis elegans* insulin-like peptide, INS-18. *Biochem Biophys Res Commun* 423: 478–483
- Mayer EA (2011) Gut feelings: the emerging biology of gut-brain communication. *Nat Rev Neurosci* 12: 453–466
- Murphy CT, Hu PJ (2013) Insulin/insulin-like growth factor signaling in *C. elegans*. *WormBook* 1–43
- Nassel DR, Winther AM (2010) *Drosophila* neuropeptides in regulation of physiology and behavior. *Prog Neurobiol* 92: 42–104
- Noma K, Jin Y (2015) Optogenetic mutagenesis in *Caenorhabditis elegans*. *Nat Commun* 6: 8868
- Nonet ML, Staunton JE, Kilgard MP, Fergestad T, Hartwig E, Horvitz HR, Jorgensen EM, Meyer BJ (1997) *Caenorhabditis elegans* rab-3 mutant synapses exhibit impaired function and are partially depleted of vesicles. *J Neurosci* 17: 8061–8073
- Nonet ML, Saifee O, Zhao H, Rand JB, Wei L (1998) Synaptic transmission deficits in *Caenorhabditis elegans* synaptobrevin mutants. *J Neurosci* 18: 70–80
- Ogg S, Ruvkun G (1998) The *C. elegans* PTEN homolog, DAF-18, acts in the insulin receptor-like metabolic signaling pathway. *Mol Cell* 2: 887–893
- Ogura K, Shirakawa M, Barnes TM, Hekimi S, Ohshima Y (1997) The UNC-114 protein required for axonal elongation and guidance in *Caenorhabditis elegans* interacts with the serine/threonine kinase UNC-51. *Genes Dev* 11: 1801–1811
- Palouzier-Paulignan B, Lacroix MC, Aime P, Baly C, Caillol M, Congar P, Julliard AK, Tucker K, Fadool DA (2012) Olfaction under metabolic influences. *Chem Senses* 37: 769–797
- Park D, Hahm JH, Park S, Ha G, Chang GE, Jeong H, Kim H, Kim S, Cheong E, Paik YK (2017) A conserved neuronal DAF-16/FoxO plays an important role in conveying pheromone signals to elicit repulsion behavior in *Caenorhabditis elegans*. *Sci Rep* 7: 7260
- Pierce SB, Costa M, Wisotzkey R, Devadhar S, Homburger SA, Buchman AR, Ferguson KC, Heller J, Platt DM, Pasquinelli AA, Liu LX, Doberstein SK, Ruvkun G (2001) Regulation of DAF-2 receptor signaling by human insulin and *ins-1*, a member of the unusually large and diverse *C. elegans* insulin gene family. *Genes Dev* 15: 672–686
- Ritter AD, Shen Y, Fuxman Bass J, Jeyaraj S, Deplancke B, Mukhopadhyay A, Xu J, Driscoll M, Tissenbaum HA, Walhout AJ (2013) Complex expression dynamics and robustness in *C. elegans* insulin networks. *Genome Res* 23: 954–965
- Root CM, Ko KI, Jafari A, Wang JW (2011) Presynaptic facilitation by neuropeptide signaling mediates odor-driven food search. *Cell* 145: 133–144
- Saeki S, Yamamoto M, Iino Y (2001) Plasticity of chemotaxis revealed by paired presentation of a chemoattractant and starvation in the nematode *Caenorhabditis elegans*. *J Exp Biol* 204: 1757–1764
- Sawin ER, Ranganathan R, Horvitz HR (2000) *C. elegans* locomotory rate is modulated by the environment through a dopaminergic pathway and by experience through a serotonergic pathway. *Neuron* 26: 619–631
- Sengupta P (2013) The belly rules the nose: feeding state-dependent modulation of peripheral chemosensory responses. *Curr Opin Neurobiol* 23: 68–75
- Shen K, Bargmann CI (2003) The immunoglobulin superfamily protein SYG-1 determines the location of specific synapses in *C. elegans*. *Cell* 112: 619–630
- Sieburth D, Ch'ng Q, Dybbs M, Tavazoie M, Kennedy S, Wang D, Dupuy D, Rual JF, Hill DE, Vidal M, Ruvkun G, Kaplan JM (2005) Systematic analysis of genes required for synapse structure and function. *Nature* 436: 510–517
- Sieburth D, Madison JM, Kaplan JM (2007) PKC-1 regulates secretion of neuropeptides. *Nat Neurosci* 10: 49–57
- Trent C, Tsuing N, Horvitz HR (1983) Egg-laying defective mutants of the nematode *Caenorhabditis elegans*. *Genetics* 104: 619–647
- Tsunozaki M, Chalasani SH, Bargmann CI (2008) A behavioral switch: cGMP and PKC signaling in olfactory neurons reverses odor preference in *C. elegans*. *Neuron* 59: 959–971
- White JG, Southgate E, Thomson JN, Brenner S (1986) The structure of the nervous system of the nematode *Caenorhabditis elegans*. *Philos Trans R Soc Lond B Biol Sci* 314: 1–340